Published in final edited form as:
Magn Reson Med. 2009 June ; 61(6): 1388–1395. doi:10.1002/mrm.21963.

Whole-Heart Contrast-Enhanced Coronary Magnetic Resonance Angiography using Gradient Echo Interleaved EPI

Himanshu Bhat[1], **Sven Zuehlsdorff**[2], **Xiaoming Bi**[2], and **Debiao Li**[1]

[1] Departments of Radiology and Biomedical Engineering, Northwestern University, Chicago, IL

[2] Siemens Medical Solutions USA, Inc., Chicago, IL

Abstract

Whole-heart coronary magnetic resonance angiography (MRA) is a promising method for detecting coronary artery disease. However, the imaging time is relatively long (on the order of 10–15 minutes). Such a long imaging time may result in patient discomfort and compromise the robustness of whole-heart coronary MRA due to increased respiratory and cardiac motion artifacts. The goal of this study was to optimize a gradient echo interleaved EPI (GRE-EPI) acquisition scheme for reducing the imaging time of contrast-enhanced whole-heart coronary MRA. Numerical simulations and phantom studies were used to optimize the GRE-EPI sequence parameters. Healthy volunteers were scanned with both the proposed GRE-EPI sequence and a 3D TrueFISP sequence for comparison purposes. Slow infusion (0.5 cc/sec) of Gd-DTPA was used to enhance the SNR of the GRE-EPI acquisition. Whole-heart images with the GRE-EPI technique were acquired with a true resolution of $1.0 \times 1.1 \times 2.0$ mm^3 in an average scan time of 4.7 ± 0.7 minutes with an average navigator efficiency of $44 \pm 6\%$. The GRE-EPI acquisition showed excellent delineation of all the major coronary arteries with scan time reduced by a factor of 2 compared with the TrueFISP acquisition.

Keywords

coronary arteries; magnetic resonance angiography; interleaved EPI; contrast media

INTRODUCTION

Whole-heart coronary MRA (1) acquires a thick axial slab covering the entire heart and allows the coronary arteries to be imaged in a single acquisition. This is different from the traditional volume-targeted approaches (2,3) in which a thin targeted slab is independently prescribed for each coronary artery. The whole-heart approach has several advantages over the volume-targeted approach. It eliminates the necessity of localization of the coronary arteries and substantially improves the workflow of coronary MRA. Furthermore, retrospective reconstruction of arbitrary views for an optimal visualization of each vessel is possible. However, the whole-heart approach is challenging due to the relatively long data acquisition time on the order of 10–15 minutes (1,4–9). Drifts in diaphragm position, patient motion and heart rate variations over these long imaging times may compromise the robustness of whole-heart coronary MRA and result in imaging artifacts (10).

Echo planar imaging (EPI) is one of the data acquisition strategies which can be used to reduce the imaging time of whole-heart coronary MRA, but this technique is sensitive to

Please send proof and correspondence to: Debiao Li, Ph.D., 737 N. Michigan Ave., Suite 1600, Chicago, IL 60611, Tel: (312) 926-4245, Fax: (312) 896-5665, Email: d-li2@northwestern.edu.

flow and off-resonance artifacts. Gradient echo interleaved EPI (GRE-EPI) (11) is a hybrid technique that provides a trade-off between scanning efficiency and artifacts and has previously been successfully applied to coronary MRA (12–16). One of the limitations in coronary MRA with GRE-EPI is the low SNR. To circumvent this problem, previous studies (12,13) used only 1 or 2 RF excitations per heart-beat using a high flip angle of 40 to 90°. This approach maximized SNR but prolonged the scan time since only a few k-space lines were acquired in each heart beat. Another study (14) used multiple RF excitations per heart-beat with a shorter TR and low flip angles of 20 to 30°, in conjunction with a T1 shortening contrast agent. As a result, the SNR was increased by minimizing the blood signal saturation. However, this study was completed during first pass of the contrast agent in a single breath hold and thus had limited slab coverage and resolution. Recently, an inversion recovery prepared conventional gradient echo sequence using slow infusion of contrast agent (17) was proposed for contrast-enhanced whole-heart coronary MRA.

The purpose of this work was to optimize a GRE-EPI acquisition scheme for reducing the imaging time of contrast-enhanced whole-heart coronary MRA. Numerical simulations and phantom studies were used to optimize the GRE-EPI sequence parameters. Healthy volunteers were scanned with both the proposed GRE-EPI sequence and a 3D TrueFISP sequence for comparison purposes. Slow infusion of an extravascular, paramagnetic contrast agent, gadopentetate dimeglumine (Gd-DTPA) was used to enhance the SNR of the whole-heart GRE-EPI acquisition.

MATERIALS AND METHODS

7 healthy volunteers (4 male and 3 female, average age 34 ± 13.2 years) were scanned on a clinical 1.5T scanner (MAGNETOM Espree, Siemens AG Healthcare Sector, Erlangen, Germany). Gd-DTPA (Magnevist, Bayer Schering Pharma, Berlin, Germany) was used as the contrast agent. Written consent was obtained from volunteers in compliance with the Institutional Review Board of our institution. All simulations were performed in the Matlab environment (Mathworks, Natick, Massachusetts, USA).

Sequence Design Considerations and Reordering Scheme

A schematic of the 3D GRE-EPI sequence is shown in Fig. 1a. Blood myocardium contrast was achieved with (a) T1 weighting using inversion recovery preparation for contrast-enhanced imaging or (b) T2 weighting using T2-preparation (18) for precontrast imaging. Fat saturation was applied prior to data acquisition. The sequence was ECG-triggered and respiratory-gated using the navigator approach. To restore the magnetization for the navigator echo, a selective reinversion (SR) pulse was applied after the nonselective inversion pulse. 6 echoes were collected after each RF pulse by blipping the phase encoding gradient, and the k-space was filled in an interleaved fashion. Both the phase and partition encoding gradients were rewound and the readout gradient was spoiled at the end of each TR. The echo train length was empirically optimized and was similar to those used in previous studies (13,14,16). A bipolar EPI readout was used to maximize scan efficiency. First order phase correction was applied for echo alignment (19). Asymmetric k-space sampling was used in the phase encoding direction in order to achieve a shorter echo time to minimize off-resonance and flow artifacts. Partial Fourier reconstruction was used to synthesize the unacquired k-space region (20).

For contrast-enhanced whole-heart coronary MRA using the described GRE-EPI sequence two predominant sources of signal modulations that result in image artifacts can be identified: i) the contrast dynamics of the slow infusion protocol and ii) signal decay within each heart beat during data acquisition.

i) Contrast agent dynamics and reordering—Typical imaging time for the GRE-EPI sequence during slow infusion of contrast agent is 4–5 minutes. Blood T1 is dynamically changing over this time, resulting in signal modulations. An efficient strategy to avoid discontinuous signal distribution in k-space was described by Bi et al (17) and is used in this study. Segmentation and interleaving were both applied along the phase encoding direction, eliminating discrete signal variations in the partition encoding direction. The reordering scheme used in the phase encoding direction is shown in Fig. 1b. The asymmetric k-space was divided into 6 regions corresponding to the echo train length, using the second region as central k-space region. The interleaved acquisition within a heart beat initially samples the lower portion of each region (shown as the dashed line) and subsequently sequentially acquires the central k-space line ($k_y = 0$) and top of each region (dotted line).

ii) Signal Decay within each heart beat—The MR signal varies within each heartbeat due to non steady state condition. In combination with the described reordering scheme, this results in amplitude discontinuities in k-space. These amplitude discontinuities lead to ghosting in the image (11). The application of dummy pulses or variable flip angle excitation for steady state preparation has been proposed to minimize these discontinuities (11). For contrast-enhanced whole-heart coronary MRA, variable flip angle series is difficult since the T1 of blood is dynamically changing. Unfortunately, dummy pulses will reduce the SNR and effectiveness of fat saturation. In this study, the amplitude modulations in the phase encoding direction were minimized by appropriate selection of the inversion time (TI) and flip angle, using simulations of the Bloch equations and phantom studies.

Simulations and Phantom Studies

The goal of the simulation was to select the scan parameters (TI and flip angle) that minimize the signal modulations and resulting image artifacts. The parameters used for the simulations were similar to the imaging parameters described below. An RR interval of 800 ms was used. To ensure steady state conditions, data was extracted using the 5^{th} heart-beat. Typical imaging time for the GRE-EPI sequence during slow infusion of contrast agent is 4–5 minutes. The T1 of blood and myocardium is dynamically changing during this time. Thus, the scan parameters were not optimized for any particular blood and myocardium T1 value. The T1 value was varied from 50 to 1200 ms and scan parameters were selected such that the sequence behavior was robust over this wide range of T1 values. A phantom containing vials of different T1 values ranging from 70 to 1500 ms was also used to visualize the artifacts caused by the modulations and to verify parameters predicted by the simulations.

Volunteer Studies

Precontrast imaging—A T2-prepared GRE-EPI sequence was used to acquire whole-heart coronary MRA prior to contrast injection. Parameters for the GRE-EPI sequence were: TR = 11.3 ms, TE = 4.2 ms, 6 echoes after each RF pulse, flip angle = 20°, readout bandwidth = 977 Hz/pixel, T2-prep duration = 40 ms, 54 to 72 lines per heartbeat in a data acquisition window of 102 to 135 ms, number of acquired k space lines = 108 to 144, FOV: 265 × 182–232 × 112–120 mm^3 matrix size: 256 × 160–204 × 56–60, voxel size: 1.0 × 1.1 × 2.0 mm^3 interpolated to 0.5 × 0.55 × 1 mm^3. The total imaging time for the GRE-EPI whole-heart scan was 2 minutes (for a heart-rate of 60 bpm without any navigator gating).

For comparison, a 3D segmented TrueFISP whole-heart scan was acquired using matched protocols with respect to data acquisition time and spatial resolution. The TrueFISP scan was accelerated using a combination of partial Fourier and parallel imaging techniques. Parameters for the TrueFISP sequence were: TR = 4.1 ms, TE = 2.0 ms, flip angle = 70°, T2-prep duration = 40 ms, 25 to 33 lines per heartbeat in a data acquisition window of 102

to 135 ms, readout bandwidth = 871 Hz/pixel, partial Fourier factor of 6/8 and GRAPPA (21) acceleration factor of 3 in the phase encoding direction. The matrix size and resolution were the same as the GRE-EPI acquisition.

In addition, for a qualitative comparison, a well established whole-heart TrueFISP protocol (1) with longer scan time, representing the state of the art for coronary MRA was performed on 2 of the volunteers. The parameters for this scan were the same as the previous TrueFISP scan, except that no partial Fourier encoding was used and the acceleration factor was reduced to 2.

For all the scans, a four chamber cine scan was used to determine the quiescent period for coronary artery imaging. Navigator pulses were placed on the dome of the right hemidiaphragm using a ± 3 mm acceptance window. Prospective real-time adaptive motion correction was applied with a correction factor of 0.6 in the superior inferior direction (22).

Contrast-enhanced Imaging—The GRE-EPI protocol was the same as described for precontrast imaging; only the T2-prep pulse was replaced by a nonselective inversion pulse with a TI of 300 ms, and the flip angle was increased from 20 to 25°. 0.2 mmol/kg body weight of Gd-DTPA was injected at a rate of 0.5 cc/sec followed by a flush of saline using the same amount and rate. The injection rate was higher than the previously published rate of 0.3cc/sec (17). This was possible due to the reduced imaging time of the GRE-EPI acquisition. For maximal SNR, a previously described method was used to trigger the scan during peak contrast enhancement (23). The partitions were acquired in a centric fashion in order to acquire the central k-space lines during peak signal enhancement. The flip angles and inversion time used in the precontrast and contrast-enhanced GRE-EPI protocols were selected based on the results of the simulation and phantom studies described in the results section.

Image Reformatting and Data Analysis—Whole-heart coronary MRA images were reformatted using the CoronaViz software (Siemens Corporate Research, Inc., Princeton, NJ, USA) to project multiple vessel branches onto a single image (24). Blood SNR and blood-myocardium CNR were evaluated in the precontrast and contrast-enhanced GRE-EPI images. Blood signal was measured as the mean value in a region of interest (ROI) (~ 1.2 cm^2) in the ascending aorta at the level of the left mail (LM) or right coronary artery (RCA). Myocardial signal was measured as the mean value in a ROI (~ 0.9 cm^2) in the tissue adjacent to left anterior descending coronary artery (LAD). Image noise was estimated as the standard deviation in a ROI (~ 1.5 cm^2) in the background air. SNR of blood was calculated as the ratio of blood signal to noise standard deviation. CNR between blood and myocardium was calculated as the difference between blood and myocardium signals divided by the noise standard deviation (25).

The contrast-enhanced GRE-EPI images were compared with the TrueFISP images acquired in the same scan time. SNR and CNR comparisons were not performed due to the spatially varying noise profiles in the GRAPPA reconstructed TrueFISP images. Image quality scores between the 2 techniques were compared. Image quality was evaluated by two independent, experienced observers who were blinded to the technique. All image quality assessments were based on the raw images. The image quality was graded as 1, poor (non-assessable); 2, fair (mild to moderate artifacts); 3, good (minimum to mild artifacts); 4, excellent (minimum or no artifacts). In addition, the lengths of the coronary arteries visualized by the 2 techniques were compared. Curved multi planar reconstructions were performed on the wholeheart datasets to delineate the LM and LAD and RCA. Each artery was manually traced over multiple slices and displayed in a single 2D image from which the vessel lengths were measured.

RESULTS

Simulations for Flip Angle and Inversion Time Optimization

For precontrast imaging (without the inversion pulse), the flip angle was varied from 15 to 30° and the resulting modulation level is shown in Fig. 2a. The modulation level is defined as the amount of signal variation within the data acquisition window in a heartbeat. For all T1 values, the modulation level increases with flip angle. Fig. 3a and b shows the phantom images for flip angles of 20 and 25° respectively. In Fig 3a there are no visible ghosting artifacts, however in Fig. 3b some ghosting artifacts are visible. Based on these results, for precontrast imaging, a flip angle of 20° should minimize the artifacts. From Fig. 2a, for a flip angle of 20° (bold line), it is seen that a modulation level less than a threshold of about 9% results in practically artifact free images. This result was used for the rest of the simulation studies to select the TI and flip angle for contrast-enhanced imaging.

Fig 2b shows the modulation for a flip angle of 20° and different inversion times. A TI of 300 ms (bold line) gives a modulation level less that 5% for the range of T1 values considered in this simulation. However, the modulation level is well below the acceptable threshold of 9%. Thus, it is possible to further increase the flip angle. Fig. 2c shows the modulation level for a TI of 300 ms and flip angle from 20 to 30°. Once again, the modulation level increases with flip angle. For a flip angle of 25° (bold line), the modulation level is always below the 9% threshold, but for a flip angle of 30° (solid line) the modulation increases to more than 10% for a T1 less than 200 ms. Fig. 2d shows the signal intensity for a TI of 300 ms and flip angles 20 to 30°. An increase in flip angle from 20 to 25° gives a substantial increase in signal; however for a flip angle of 30°, the increase in signal is small. Based on these results, a TI of 300 ms and a flip angle of 25° should minimize ghosting artifacts and give high signal. Fig. 3c and d shows the phantom images for a TI of 300 ms and flip angles 25 and 30° respectively. In Fig 3c there are no visible ghosting artifacts, however in Fig. 3d some ghosting artifacts are visible. The phantom images confirm the results of the simulations and demonstrate the robustness of the chosen TI (300 ms) and flip angle (25°).

Volunteer Studies

All the volunteer studies were successfully completed. Compared to precontrast imaging using T2-prep, the SNR was increased by 78% (precontrast/contrast-enhanced: 13.3/23.7), and CNR was increased by 169% (precontrast/contrast-enhanced: 4.8/12.9) for the contrast-enhanced GRE-EPI acquisition. The average imaging time for contrast-enhanced whole-heart imaging was 4.7 ± 0.7 minutes with an average navigator efficiency of 44 ± 6.2%.

Fig. 4 shows reformatted coronary artery images from 3 volunteers using the contrast-enhanced GRE-EPI acquisition (4a, c and e) and the TrueFISP acquisition with identical imaging time (4b, d and f). The contrast-enhanced GRE-EPI acquisition shows excellent depiction of all the coronary arteries. In comparison, the TrueFISP acquisition is very noise due to the noise enhancement as a result of the high acceleration factor used. The quantitative comparison between the two sequences is shown in Table 1. The average imaging times and navigator efficiencies were similar for both acquisitions. The average image quality score for the contrast-enhanced GRE-EPI sequence was 2.97 ± 0.3, compared to 2.21 ± 0.3 for the TrueFISP sequence. The difference between them was statistically significant (p value = 0.001). The average visualized vessel length of the RCA was significantly higher for the GRE-EPI sequence (p value = 0.01). The average visualized length of the LAD was higher for the GRE-EPI sequence, but the difference was not statistically significant (p value = 0.4).

Fig. 5 shows reformatted coronary artery images from 2 more volunteers using the contrast-enhanced GRE-EPI acquisition and the TrueFISP acquisition with an acceleration factor of 2 (leading to longer imaging time). The imaging times for the contrast-enhanced GRE-EPI acquisition (5a, c and e) were 5.6 and 5.7 minutes with navigator efficiencies of 45 and 33 % respectively. The imaging times for the TrueFISP acquisition (5b, d and f) were 13.2 and 8.4 minutes with navigator efficiencies of 38 and 47 % respectively. Both the sequences show similar depiction of the coronary arteries; however the imaging time for the contrast-enhanced GRE-EPI acquisition is reduced by a factor of 2 compared with the TrueFISP acquisition.

DISCUSSION

In this study, contrast-enhanced whole-heart coronary artery images were acquired in less than 5 minutes using a GRE-EPI sequence. This is more than a factor of 2 reduction compared with previous protocols reported at both 1.5T and 3T (1,4–6,9). The short scan time minimizes image artifacts due to changes in breathing pattern, patient motion and variations in heart rate, since these effects tend to increase with scan time (10). It should also lead to increased patient comfort.

A high readout bandwidth of 977 Hz/pixel compared with previous FLASH studies (17,26) was used in order to maximize the phase encoding bandwidth, which is related to the EPI ghosting artifacts in the phase encoding direction (11). The low signal due to the high bandwidth was compensated by multiple mechanisms. First, the EPI readout resulted in a long TR of 11.3 ms, which leads to a higher steady state signal compared with a shorter TR of 3 to 4 ms. Second, the longer TR allowed the use of a flip angle of 25° without any signal modulation and saturation effects. Third, the shorter scan time made it possible to increase the contrast injection rate from the previously proposed 0.3 cc/sec (17) to 0.5 cc/sec. Fourth, a previously described method (23) was used to trigger the scan during peak contrast enhancement.

Previous contrast-enhanced coronary MRA studies (17,26,27) have used flip angles in the range of 20 to 25° for typical repetitions times between 3 and 4 ms. Based on these results, for a TR of 11.3 ms, a flip angle of higher than 25° used in this study should be possible. However, the signal decay within each heart-beat due to non steady state conditions, in combination with the interleaved EPI readout leads to amplitude discontinuities in the phase-encoding direction. In this work, based on simulations and phantom studies, the inversion time and flip angle were chosen to give practically artifact free images in the presence of these discontinuities. A more complete optimization of parameters would have been possible if the exact blood and myocardium T1 values after slow infusion of contrast agent were known. The blood and myocardium T1 changes after a bolus injection have been reported (28). To our knowledge no such study exists for slow infusion of contrast agent. However, based on the volunteer studies, the selected TI and flip angle gave artifact free images and resulted in high blood SNR and blood myocardium CNR.

The contrast-enhanced GRE-EPI sequence was compared with the TrueFISP technique, which is the current gold standard for coronary MRA at 1.5T. To match the scan time for the 2 techniques, the TrueFISP scan was performed with an acceleration factor of 3 in the phase encoding direction. This is higher than the traditionally used acceleration factor of 2 (1). This resulted in significant noise enhancement in the reconstructed images. As a result, the GRE-EPI sequence had significantly better image quality than the TrueFISP scan. Additionally, for a qualitative comparison, a well established TrueFISP protocol (1) with an acceleration factor of 2 and longer scan time was acquired in 2 of the volunteers. The coronary artery depiction in the GRE-EPI sequence was very similar to the TrueFISP scan in

both the volunteers. These comparisons show that the GRE-EPI sequence gives similar image quality and coronary artery delineation in a shorter scan time.

One of the disadvantages of interleaved EPI is its sensitivity to flow, off-resonance and cardiac motion artifacts. Various techniques have been proposed for dealing with flow and motion for EPI. Ref (29) proposed flyback EPI for flow compensation in the readout direction and gradient moment nulling for compensating the phase- and partition-encoding directions. This technique reduces the scan efficiency and was not used in our study. Another study (30) showed that center-out EPI with partial flyback is robust in the presence of flow, due to the use of both, flyback and the shortest possible TE. But, center-out EPI is more sensitive to off-resonance artifacts and amplitude modulations. As a result, in this study we used partial Fourier acquisition to limit the TE to 4.2 ms. and TR to 11.3 ms. These values fall within the range of 10–15 ms reported in Refs (31,32) for producing artifact free interleaved EPI images in the heart at 1.5T. Consistent with their findings, we did not see any visible off-resonance or flow artifacts, including ghosts and signal voids. However, the T2* decay is expected to introduce some blurring in the EPI images. This is a trade-off for using EPI and is partially offset by the fact that the shorter imaging time imaging makes it less likely to have navigator drifts and results in fewer respiratory motion artifacts. Another drawback of using interleaved EPI is that, compared to a non EPI acquisition, more time is spent sampling the central k-space region within the data acquisition window in a heartbeat. As a result, it is critical to carefully select the acquisition window to avoid any cardiac motion artifacts. In patient studies, it may be necessary to select a slight shorter window to accommodate heart-rate changes during the scan. Another generic limitation of contrast-enhanced studies is that it is difficult to repeat the scan if the results are not adequate. Also, with the recent concerns of nephrogenic systemic fibrosis (33) it might not be applicable in all patients.

Recently, whole-heart TrueFISP acquisition with high acceleration factors in conjunction with high density receive coil arrays has been reported (34). The use of 32 or higher channel MR systems for the GRE-EPI acquisition should allow for combining parallel imaging and EPI, for a further reduction in the scan time. For combining EPI and parallel imaging, the use of auto-calibration introduces different traversal velocities in different k-space regions (35) resulting in image artifacts, so external calibration should be explored.

Application of GRE-EPI at 3T should also be investigated, since the higher SNR could be traded for further reduction in scan time. GRE-EPI at 3T needs to overcome some of the following problems: i) the off-resonance phase impedes accurate determination of the linear and constant phase differences between the even and odd echoes ii) fat saturation, which is critical for both EPI and Coronary MRA, is a problem due to the B_0 and B_1 inhomogeneities and iii) the echo train length needs to be optimized due to decreased T2*.

In conclusion, a GRE-EPI sequence was optimized for contrast-enhanced whole-heart coronary MRA at 1.5 Tesla. In healthy volunteers, all the major coronary arteries were clearly depicted in a scan time under 5 minutes. Clinical utility of the technique needs to be tested on a patient population.

Acknowledgments

The authors thank Xin Liu, M.D. for scoring the images and Jessy Mouannes for providing the phantom with different T1 values.

Supported in part by National Institute of Health grants nos. NIBIB EB002623 and NHLBI HL38698, and Siemens Medical Solutions USA, Inc., Malvern, PA.

References

1. Weber OM, Martin AJ, Higgins CB. Whole-heart steady-state free precession coronary artery magnetic resonance angiography. Magn Reson Med. 2003; 50(6):1223–1228. [PubMed: 14648570]
2. Wielopolski PA, van Geuns RJ, de Feyter PJ, Oudkerk M. Breath-hold coronary MR angiography with volume-targeted imaging. Radiology. 1998; 209(1):209–219. [PubMed: 9769834]
3. van Geuns RJ, Wielopolski PA, Wardeh AJ, de Bruin HG, Oudkerk M, de Feyter PJ. Volume coronary angiography using targeted scans (VCATS): a new strategy in MR coronary angiography. Int J Cardiovasc Imaging. 2001; 17(5):405–410. [PubMed: 12025954]
4. Sakuma H, Ichikawa Y, Chino S, Hirano T, Makino K, Takeda K. Detection of coronary artery stenosis with whole-heart coronary magnetic resonance angiography. J Am Coll Cardiol. 2006; 48(10):1946–1950. [PubMed: 17112982]
5. Gharib AM, Ho VB, Rosing DR, Herzka DA, Stuber M, Arai AE, Pettigrew RI. Coronary artery anomalies and variants: technical feasibility of assessment with coronary MR angiography at 3 T. Radiology. 2008; 247(1):220–227. [PubMed: 18372470]
6. Stuber M, Weiss RG. Coronary magnetic resonance angiography. J Magn Reson Imaging. 2007; 26(2):219–234. [PubMed: 17610288]
7. Stehning C, Boernert P, Nehrke K. Advances in coronary MRA from vessel wall to whole heart imaging. Magn Reson Med Sci. 2007; 6(3):157–170. [PubMed: 18037796]
8. Yang, Q.; Li, D.; Bi, X.; An, J.; Zhang, Q.; Jerecic, R.; Li, K. Diagnostic Value of Contrast-Enhanced Whole-heart Coronary MRA at 3.0Tesla. Proceedings of the 16th Annual Meeting of ISMRM; Toronto, Canada. 2008. p. 315
9. Liu X, Bi X, Huang J, Jerecic R, Carr J, Li D. Contrast-enhanced whole-heart coronary magnetic resonance angiography at 3.0 T: comparison with steady-state free precession technique at 1.5 T. Invest Radiol. 2008; 43(9):663–668. [PubMed: 18708861]
10. Chang S, Cham MD, Hu S, Wang Y. 3-T navigator parallel-imaging coronary MR angiography: targeted-volume versus whole-heart acquisition. AJR Am J Roentgenol. 2008; 191(1):38–42. [PubMed: 18562722]
11. McKinnon GC. Ultrafast interleaved gradient-echo-planar imaging on a standard scanner. Magn Reson Med. 1993; 30(5):609–616. [PubMed: 8259061]
12. Bornert P, Jensen D. Coronary artery imaging at 0.5 T using segmented 3D echo planar imaging. Magn Reson Med. 1995; 34(6):779–785. [PubMed: 8598804]
13. Botnar RM, Stuber M, Danias PG, Kissinger KV, Manning WJ. A fast 3D approach for coronary MRA. J Magn Reson Imaging. 1999; 10(5):821–825. [PubMed: 10548794]
14. Deshpande VS, Wielopolski PA, Shea SM, Carr J, Zheng J, Li D. Coronary artery imaging using contrast-enhanced 3D segmented EPI. J Magn Reson Imaging. 2001; 13(5):676–681. [PubMed: 11329188]
15. Slavin GS, Riederer SJ, Ehman RL. Two-dimensional multishot echo-planar coronary MR angiography. Magn Reson Med. 1998; 40(6):883–889. [PubMed: 9840833]
16. Wielopolski PA, Manning WJ, Edelman RR. Single breath-hold volumetric imaging of the heart using magnetization-prepared 3-dimensional segmented echo planar imaging. J Magn Reson Imaging. 1995; 5(4):403–409. [PubMed: 7549201]
17. Bi X, Carr JC, Li D. Whole-heart coronary magnetic resonance angiography at 3 Tesla in 5 minutes with slow infusion of Gd-BOPTA, a high-relaxivity clinical contrast agent. Magn Reson Med. 2007; 58(1):1–7. [PubMed: 17659628]
18. Brittain JH, Hu BS, Wright GA, Meyer CH, Macovski A, Nishimura DG. Coronary angiography with magnetization-prepared T2 contrast. Magn Reson Med. 1995; 33(5):689–696. [PubMed: 7596274]
19. Bruder H, Fischer H, Reinfelder HE, Schmitt F. Image reconstruction for echo planar imaging with nonequidistant k-space sampling. Magn Reson Med. 1992; 23(2):311–323. [PubMed: 1549045]
20. Noll DC, Nishimura DG, Macovski A. Homodyne detection in magnetic resonance imaging. IEEE Trans Med Imaging. 1991; 10(2):154–163. [PubMed: 18222812]

21. Griswold MA, Jakob PM, Heidemann RM, Nittka M, Jellus V, Wang J, Kiefer B, Haase A. Generalized autocalibrating partially parallel acquisitions (GRAPPA). Magn Reson Med. 2002; 47(6):1202–1210. [PubMed: 12111967]
22. Wang Y, Ehman RL. Retrospective adaptive motion correction for navigator-gated 3D coronary MR angiography. J Magn Reson Imaging. 2000; 11(2):208–214. [PubMed: 10713956]
23. Bhat, H.; Lai, P.; Li, D. Real Time Self Tracking of Contrast Kinetics for Whole Heart Coronary Artery Magnetic Resonance Angiography. Proceedings of the 16th Annual Meeting of ISMRM; Toronto, Canada. 2008. p. 914
24. Aharon, S.; Oksuz, O.; Lorenz, C. Simultaneous projection of multibranched vessels with their surroundings on a single image from coronary MRA. Proceedings of the 14th Annual Meeting of ISMRM; Seattle, WA, USA. 2006. p. 365
25. Stuber M, Botnar RM, Fischer SE, Lamerichs R, Smink J, Harvey P, Manning WJ. Preliminary report on in vivo coronary MRA at 3 Tesla in humans. Magn Reson Med. 2002; 48(3):425–429. [PubMed: 12210906]
26. Bi X, Li D. Coronary arteries at 3.0 T: Contrast-enhanced magnetization-prepared three-dimensional breathhold MR angiography. J Magn Reson Imaging. 2005; 21(2):133–139. [PubMed: 15666400]
27. Li D, Carr JC, Shea SM, Zheng J, Deshpande VS, Wielopolski PA, Finn JP. Coronary arteries: magnetization-prepared contrast-enhanced three-dimensional volume-targeted breath-hold MR angiography. Radiology. 2001; 219(1):270–277. [PubMed: 11274569]
28. Sharma P, Socolow J, Patel S, Pettigrew RI, Oshinski JN. Effect of Gd-DTPA-BMA on blood and myocardial T1 at 1.5T and 3T in humans. J Magn Reson Imaging. 2006; 23(3):323–330. [PubMed: 16456820]
29. Duerk JL, Simonetti OP. Theoretical aspects of motion sensitivity and compensation in echo-planar imaging. J Magn Reson Imaging. 1991; 1(6):643–650. [PubMed: 1823169]
30. Luk Pat GT, Meyer CH, Pauly JM, Nishimura DG. Reducing flow artifacts in echo-planar imaging. Magn Reson Med. 1997; 37(3):436–447. [PubMed: 9055235]
31. Reeder SB, Atalar E, Faranesh AZ, McVeigh ER. Multi-echo segmented k-space imaging: an optimized hybrid sequence for ultrafast cardiac imaging. Magn Reson Med. 1999; 41(2):375–385. [PubMed: 10080287]
32. Epstein FH, Arai AE. Optimization of fast cardiac imaging using an echo-train readout. J Magn Reson Imaging. 2000; 11(2):75–80. [PubMed: 10713937]
33. Broome DR, Girguis MS, Baron PW, Cottrell AC, Kjellin I, Kirk GA. Gadodiamide-associated nephrogenic systemic fibrosis: why radiologists should be concerned. AJR Am J Roentgenol. 2007; 188(2):586–592. [PubMed: 17242272]
34. Nehrke K, Bornert P, Mazurkewitz P, Winkelmann R, Grasslin I. Free-breathing wholeheart coronary MR angiography on a clinical scanner in four minutes. J Magn Reson Imaging. 2006; 23(5):752–756. [PubMed: 16557495]
35. Skare S, Newbould RD, Clayton DB, Albers GW, Nagle S, Bammer R. Clinical multishot DW-EPI through parallel imaging with considerations of susceptibility, motion, and noise. Magn Reson Med. 2007; 57(5):881–890. [PubMed: 17457876]

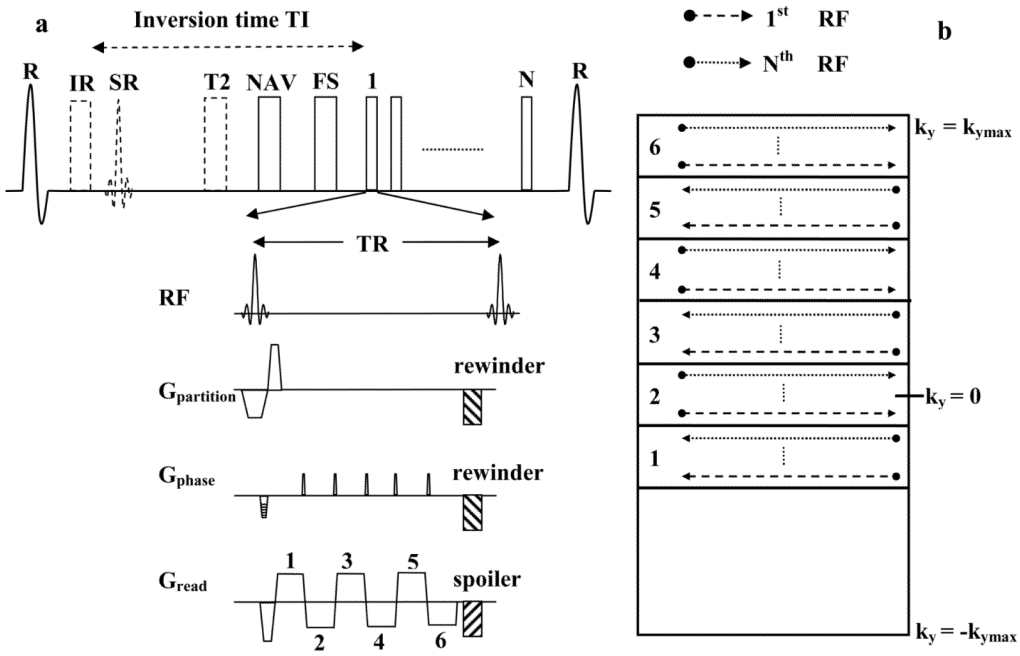

Figure 1.

Schematic of the pulse sequence and reordering scheme. 1a: Inversion Recovery (IR) or T2-prepared (T2), fat saturated (FS), ECG triggered and navigator (NAV) gated, 3D GRE-EPI sequence used for whole-heart coronary MRA. SR stands for the selective reinversion pulse which is used to restore the magnetization for the navigator echo. 1b: Reordering scheme in the phase encoding direction showing how the 6 echoes after each RF pulse fill k-space.

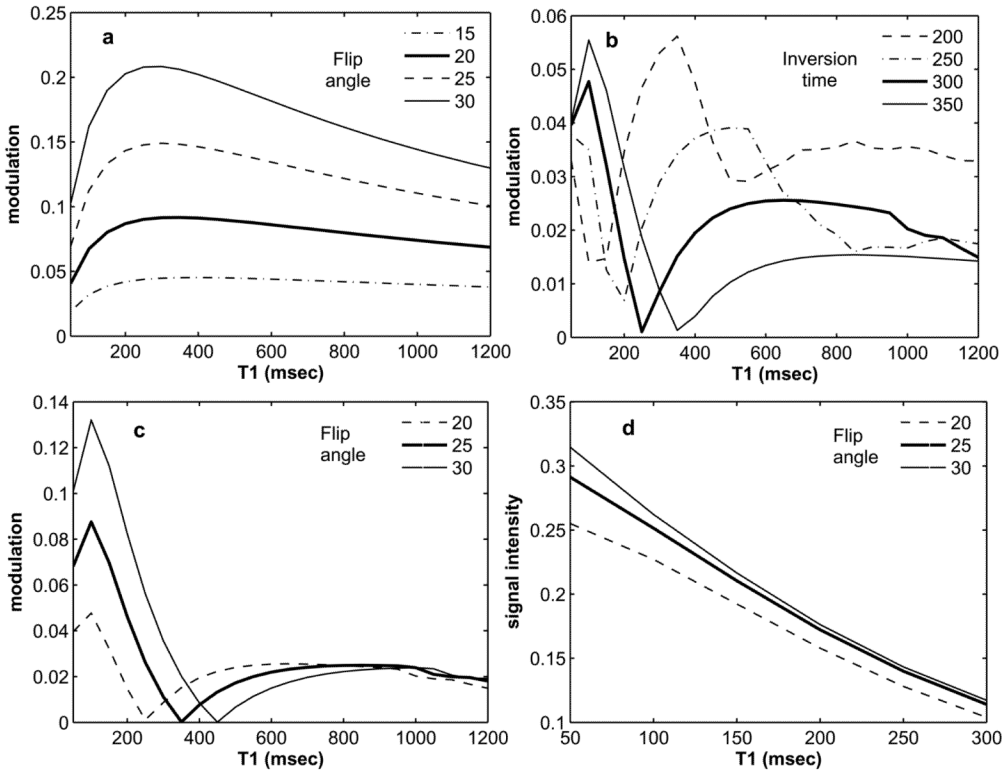

Figure 2.

Results of simulations. 2a: Modulation level for precontrast imaging with varying flip angles. 2b: Modulation level for contrast-enhanced imaging with a flip angle of 20° and varying TI. 2c: Modulation level for contrast-enhanced imaging with a TI of 300 ms and varying flip angles. 2d: Signal intensity for contrast-enhanced imaging with a TI of 300 ms and varying flip angles. Based on these simulations a flip angle of 25° and a TI of 300 ms were chosen for the contrast-enhanced volunteer studies.

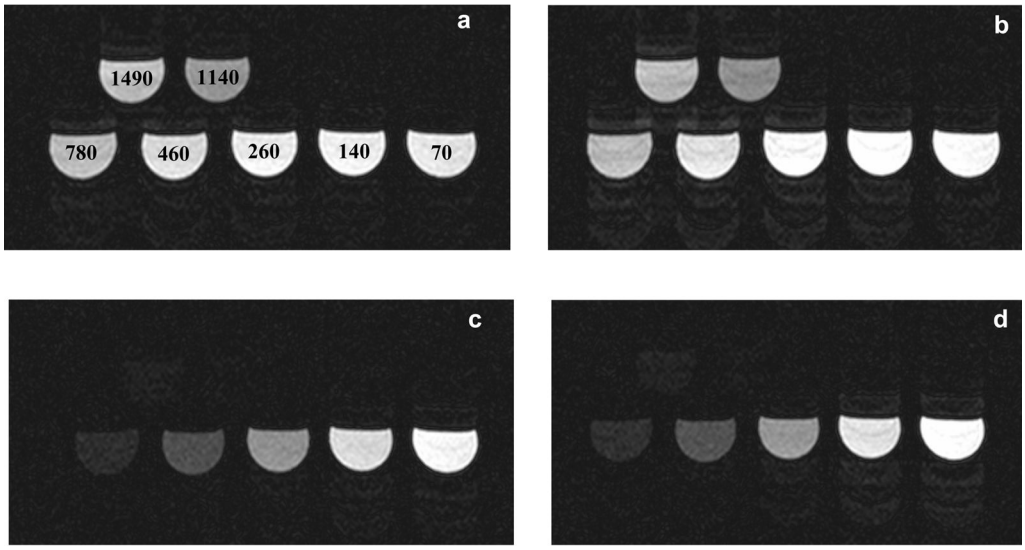

Figure 3.
Phantom images. 3a and b: Phantom images without inversion pulse for flip angles of 20 and 25° respectively. The T1 values for the vials are written on the images in 3a. 3c and d: Phantom images with inversion pulse (TI = 300 ms) for flip angles of 25 and 30° respectively. These images show the robustness of the selected flip angle (25°) and TI (300 ms) for contrast-enhanced imaging.

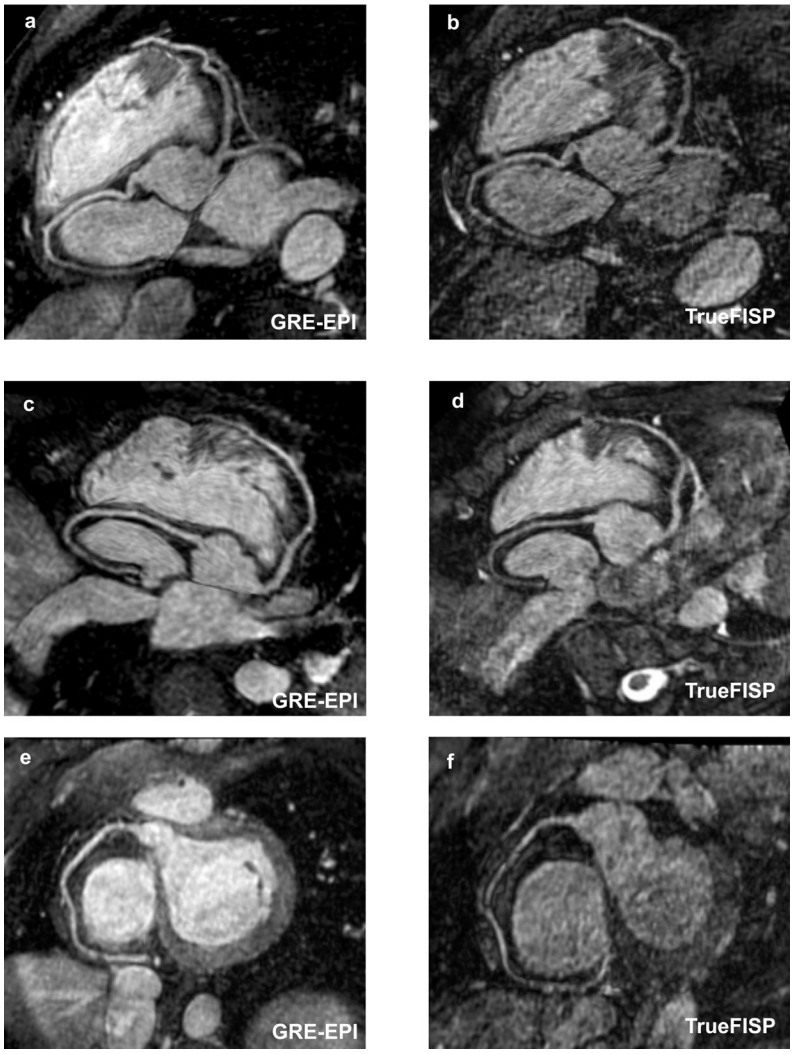

Figure 4.
Reformatted coronary artery images from 3 volunteers using the contrast-enhanced GRE-EPI acquisition (4a, c and e) and the TrueFISP acquisition with identical imaging time (4b, d and f). The contrast-enhanced GRE-EPI acquisition shows excellent depiction of the coronary arteries compared to the TrueFISP acquisition, which is very noise due to the high acceleration factor used.

Figure 5.
Reformatted coronary artery images from 2 volunteers using the contrast-enhanced GRE-EPI acquisition (5a, c and e) and the ideal TrueFISP acquisition with an acceleration factor of 2, leading to longer imaging time (5b, d and f). Both the sequences show similar depiction of the coronary arteries, however, the imaging time for the contrast-enhanced GRE-EPI acquisition is reduced by a factor of 2 compared with the TrueFISP acquisition.

Table 1

Quantitative comparison between the contrast-enhanced GRE-EPI acquisition and the TrueFISP acquisition with identical imaging times. The image quality score and RCA length were significantly higher for the contrast-enhanced GRE-EPI sequence compared to the TrueFISP sequence. The LAD length was also higher but the difference was not statistically significant.

				Vessel length (cm)	
Imaging sequence	**Imaging time (minutes)**	**Navigator efficiency (%)**	**Image quality score**	**LM + LAD**	**RCA**
Contrast-enhanced GRE-EPI	4.78 ± 0.75	44.71 ± 6.23	2.97 ± 0.30	11.52 ± 3.21	10.88 ± 2.17
TrueFISP	4.91 ± 0.92	45.57 ± 7.97	2.21 ± 0.31	11.09 ± 4.13	9.17 ± 1.72
p value (n = 7)	0.54	0.80	0.0013*	0.45	0.01*

* indicates statistically significant